Annealing effects on residual stress of HfO_2/SiO_2 multilayers

**Yanming Shen (申雁鸣)[1,2], Zhaoxia Han (韩朝霞)[3], Jianda Shao (邵建达)[1],
Shuying Shao (邵淑英)[1], and Hongbo He (贺洪波)[1]**

[1]*Shanghai Institute of Optics and Fine Mechanics, Chinese Academy of Sciences, Shanghai 201800*
[2]*Graduate University of Chinese Academy of Sciences, Beijing 100049*
[3]*School of Science, Henan University of Science and Technology, Luoyang 471003*

Received July 5, 2007

HfO_2/SiO_2 multilayer films were deposited on BK7 glass substrates by electron beam evaporation method. The effects of annealing at the temperature between 200 and 400 °C on residual stresses have been studied. It is found that the residual stress of as-deposited HfO_2/SiO_2 multilayers is compressive. It becomes tensile after annealing at 200 °C, and then the value of tensile stress increases as annealing temperature increases. And cracks appear in the film because tensile stress is too large when the sample is annealed at 400 °C. At the same time, the crystallite size increases and interplanar distance decreases with the increase of annealing temperature. The variation of residual stresses is corresponding with the evolution of structures.

OCIS codes: 230.1360, 220.0220, 310.6860.

HfO_2/SiO_2 multilayer films are widely used in optical films because of their unique optical, mechanical properties and high laser-induced damage threshold (LIDT) [1,2]. Film stress is an important parameter that must be characterized and ultimately controlled, which can cause severe problems for a number of applications in advanced technology. For instance, excessive residual stress can limit the reliability and function of thin-film-based structures due to peeling, cracking and curling[3−5]. So the control of residual stress is very crucial. Annealing is an important method to alter the properties of thin films. The objective of this study is to reveal the effects of annealing on residual stress of the HfO_2/SiO_2 multilayers, in the meantime, the relation between residual stress and structure is also discussed.

HfO_2/SiO_2 multilayer films were deposited on BK7 glass substrates by electron beam evaporation. The glass substrate had a 50-mm diameter, and its thickness was 5 mm. The coating materials with purity of 99.99% were in tablet form from Beijing General Research Institute for Nonferrous Metals. The film stacks were $(HL)^{12}$, where H and L presented HfO_2 and SiO_2, respectively. The thicknesses of a HfO_2 layer and a SiO_2 layer were 70 and 95 nm, respectively. The vacuum chamber was baked for 3 h at the temperature of 290 °C and maintained 290 °C during deposition. The deposition rates of HfO_2 and SiO_2 were 0.45 and 0.75 nm/s, respectively. The base pressure was 2.0×10^{-3} Pa, and the deposition pressure was maintained 2.0×10^{-2} Pa by filling vacuum chamber pure oxygen during HfO_2 deposition, which was adjusted to 5×10^{-3} Pa during SiO_2 deposition. The film-layer thickness was controlled by the single-wavelength turning point method with a wavelength of 550 nm. The HfO_2/SiO_2 multilayer films were annealed in the atmosphere for 2 h at selected annealing temperatures of 200, 300, and 400 °C, respectively. The heating rate was 10 °C/min and the temperature cooled naturally in the furnace.

The substrate radius of curvature was measured by ZYGO interferometer. The residual stress σ in the film is then given by[6]

$$\sigma = \frac{E_\mathrm{s}}{6(1-\nu_\mathrm{s})}\frac{t_\mathrm{s}^2}{t_\mathrm{f}}\left(\frac{1}{R}-\frac{1}{R_0}\right), \quad (1)$$

where E_s and ν_s are the Young's modulus and the Poisson's ratio of the substrate, respectively. R_0 and R are the radii of the substrate curvature before and after deposition, respectively. t_s and t_f are the thicknesses of the substrate and the film, respectively. The equipment measurement accuracy is about $\lambda/50$ ($\lambda = 632.8$ nm). Conventially, tensile stress was indicated as positive, while compressive stress was indicated as negative.

The structure of multilayers was characterized by X-ray diffraction (XRD) with 2θ angle in the range of $20° - 85°$ using a Cu $K\alpha$ radiation in a step of 0.02°. The interplanar distance d was calculated by the equation of $2d\sin\theta = \lambda$, where θ is the Bragg diffraction angle and λ is the X-ray wavelength. The crystallite size D of thin films was estimated using the formula $D = 0.9\lambda/(\beta\cos\theta)$, where $\lambda = 0.15418$ nm, β is the full width at half maximum (FWHM). The surface morphologies of samples were mapped by Nomarski microscope with magnifying multiple 200.

The values of residual stress of HfO_2/SiO_2 multilayers annealed at different temperatures are illustrated in Fig. 1. It is clear that the residual stress of as-deposited sample is compressive stress with a value of 42 MPa. It becomes tensile stress with a value of 19 MPa after annealing at 200 °C, then the value increases gradually with the increase of annealing temperature. The residual stress reaches 116 MPa after annealing at 400 °C, at the same time, several microcracks appear in local regions, as shown in Fig. 2.

The XRD spectra of HfO_2/SiO_2 multilayers annealed at different temperatures are shown in Fig. 3. It can be seen that SiO_2 layers are amorphous structure in all the

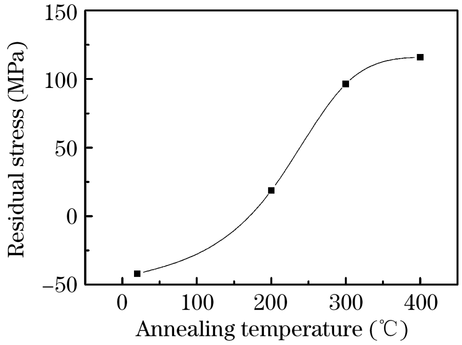

Fig. 1. Residual stress of HfO_2/SiO_2 multilayers annealed at different temperatures.

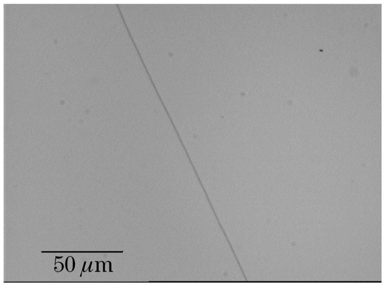

Fig. 2. Cracks in the sample annealed at 400 °C.

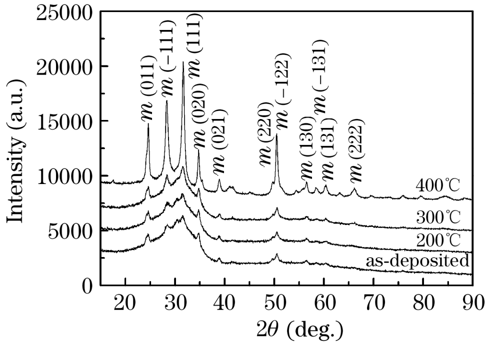

Fig. 3. XRD spectra of samples after annealing.

samples, and HfO_2 layers exhibit monoclinic. There are no evidently proffered orientations in as-deposited samples. The intensities of $m(011)$, $m(-110)$, $m(111)$ and $m(-122)$ are almost same. The spectra hardly change when the samples are annealed at 200 °C. As annealing temperature increases to 300 °C, the intensities of all peaks increase, and $m(111)$ becomes proffered orientation. The intensities of peaks increase largely when the annealing temperature increases to 400 °C, which indicates that crystallite size increases significantly. Figure 4 indicates that $m(111)$ peak shifts to right with the increase of annealing temperature. Table 1 lists some characteristics of $m(111)$ peak, where we can find that the characteristics of $m(111)$ have little differences after annealing at 200 °C. The intensity of the peak increases with the further increasing of annealing temperature, and the crystallite size increases, correspondingly. In the mean while, the peak position shifts to right and the interplanar distance decreases.

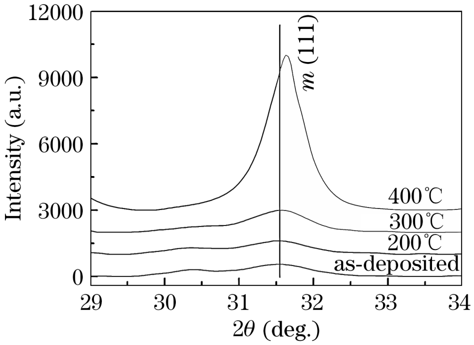

Fig. 4. Spectral shifts of $m(111)$.

The residual stress of film is composed of intrinsic stress σ_{in} and thermal stress σ_{th}[7],

$$\sigma = \sigma_{\text{in}} + \sigma_{\text{th}}. \tag{2}$$

The intrinsic stress originates from various defects and lattice mismatch between the films and substrates and depends on the method of film preparation, deposition conditions, growth rate, nature of substrate, etc.. Thermal stress is caused both by the different thermal expansion coefficients between the films and the substrates and by the temperature difference between the deposition temperature T_1 and the ambient temperature T_0. The thermal stress of multilayers can be obtained by[8]

$$\sigma_{\text{th}} = \frac{1}{t_{\text{f}}} \sum_{i=1}^{n} \frac{E_i t_i}{(1-\nu_i)} (\alpha_i - \alpha_{\text{s}})(T_1 - T_0), \tag{3}$$

where t_{f} is the total thickness of the multilayers, E_i and ν_i are the Young's modulus and the Poisson's ratio of ith layer, respectively. t_i is the thickness of ith layer. α_i and α_{s} are the thermal expand coefficients of ith layer and substrate.

It is well known that the structure of the material can be restored and recrystallized during the process of annealing. When the annealing temperature is lower, the energy offered by annealing is mainly consumed to

Table 1. Characteristics of $m(111)$ Peak of Samples Annealed at Different Temperatures

Annealing Temperature (°C)	Peak Position (deg.)	Intensity (a.u.)	Interplanar Distance (nm)	FWHM (deg.)	Crystallite Size (nm)
As Deposited	31.5418	801	0.2834	0.7822	10.6
200	31.5504	746	0.2833	0.7420	11.1
300	31.5991	1117	0.2829	0.6628	12.5
400	31.6258	6997	0.2827	0.4252	19.4

recover the film's initial structure and not enough to make the grain growth. The grain would grow significantly when enough energy is offered at higher annealing temperature. So we can see that the differences of structure are very small after annealing at 200 °C and large differences are obtained after annealing at higher temperature. The HfO_2 layers are composed of many microcrystal grains. After annealing at higher temperatures, the crystallite grain grows larger and grain boundary area decreases. The film is looser in grain boundary, and reduction of grain boundary causes film horizontal contraction, which leads to the increase of tensile stress[9]. Annealing reduces microdefects and microvoids, which can also densify the films and favor increase of tensile stress[10]. In addition, annealing can drive away water absorbed in pores and also favor increase of tensile stress. It has large influences on residual stress in SiO_2 layers[11], especially. Therefore, with the increase of annealing temperature, the residual stress becomes tensile stress from compressive stress, and the tensile stress gradually increases.

The residual stress of all samples are measured at ambient temperature. The thermal stress of multilayers can be considered unchanged before and after annealing, but it is changed during the process of annealing when the temperature varies. The thermal expansion coefficients of HfO_2 layer and SiO_2 layer are 3.6×10^{-6}/K[12] and 3.1×10^{-6}/K[12], which are lower than α_s $(7.1 \times 10^{-6}/K)$[13]. Therefore, the thermal stress of HfO_2/SiO_2 multilayers is tensile stress as the temperature increases during annealing. The thermal stress can reach 220 MPa when the sample is annealed at 400 °C, so the total stress of multilayers is so large that cracks appear in the multilayers.

In the θ-2θ mode of XRD measurement, only crystallites with lattice planes parallel to the surface are measured. As shown in Table 1, the diffraction peak of $m(111)$ moves to right as the annealing temperature increases, and the interplanar distance decreases accordingly. Tensile stress parallel to the surface causes vertical contraction of the film and decrease of interplanar distance, which are parallel to the surface. Therefore the observed decrease of interplanar distance (decrease of 2θ) indicates tensile stress, which is consistent with the measured residual stress. Therefore, the variation of residual stress can be attributed to the evolution of structure.

In conclusion, annealing is an effective method of adjusting residual stress of the films. Under our experimental conditions, the residual stress of as-deposited HfO_2/SiO_2 multilayers is compressive. It becomes tensile after annealing at 200 °C, and then the value of tensile stress increases as annealing temperature increases. Cracks appear in the films, because the tensile stress is too large when the sample is annealed at 400 °C. Annealing at proper temperature can reduce residual stress of HfO_2/SiO_2 multilayers, but exorbitant annealing temperature can induce the films to crack. The crystallite size increases with the increase of annealing temperature, and the position of $m(111)$ peak shifts to right and the interplanar distance decreases. The variation of residual stress is consistent with the change of interplanar distances.

This work was supported by the National Natural Science Foundation of China under Grant No. 10704078. Y. Shen's e-mail address is shenyanming@siom.ac.cn.

References

1. Y. Shen, S. Shao, H. He, J. Shao, and Z. Fan, Chin. Opt. Lett. **5,** S272 (2007).
2. Y. Zhao, T. Wang, D. Zhang, J. Shao, and Z. Fan, Appl. Surf. Sci. **245,** 335(2005).
3. S. Shao, J. Shao, H. He, and Z. Fan, Opt. Lett. **30,** 2119 (2006).
4. Y. Shen, H. He, S. Shao, and Z. Fan, Chin. J. Lasers (in Chinese) **33,** 827 (2006).
5. S. Shao, G. Tian, Z. Fan, and J. Shao, Acta Opt. Sin. (in Chinese) **25,** 126 (2005).
6. S. Tamulevičcius, Vacuum **51,** 127 (1998).
7. Y. Shen, H. He, S. Shao, J. Shao, and Z. Fan, High Power Laser and Particle Beams (in Chinese) **17,** 1812 (2005).
8. C. H. Hsueh, Thin Solid Films **418,** 182 (2002).
9. P. Chaudhari, J. Vac. Sci. Technol. **9,** 520 (1972).
10. H. S. Story and R. W. Hoffman, Proc. Phys. Soc. B **70,** 950 (1957).
11. H. Leplan and B. Geenen, J. Appl. Phys. **78,** 962 (1995).
12. R. Thielsch, A. Gatto, and N. Kaiser, Appl. Opt. **41,** 3211 (2002).
13. S. Shao, Z. Fan, J. Shao, and H. He, Thin Solid Films **445,** 59 (2003).